Structure & Expression, ISBN 0-940030-21-7
Volume 1: From Proteins to Ribosomes, ISBN 0-940030-21-7
Eds., R.H. Sarma & M.H. Sarma, Adenine Press, ©Adenine Press 1988.

Molecular Dynamics: Applications to Proteins

Martin Karplus, Axel T. Brünger[1], Ron Elber[2] and John Kuriyan[3]

Department of Chemistry
Harvard University
Cambridge, Massachusetts 02138

[1]Department of Molecular Biophysics & Biochemistry
Yale University
New Haven, Connecticut 06511

[2]Department of Chemistry
University of Illinois at Chicago
Chicago, Illinois 60680

[3]Laboratory of Biochemistry & Bioorganic Chemistry
Rockefeller University
New York, N.Y. 10021

I. Introduction

Molecular dynamics simulations of biomolecules have the possibility of providing the ultimate detail concerning motional phenomena (1). The primary limitation of such simulation methods is that they are approximate. It is here that experiment plays an essential role in validating the simulations; that is, comparisons with experimental data can serve to test the accuracy of the calculations and to provide criteria for improving the methodology. When experimental comparisons indicate that the simulations are meaningful, their capacity for providing detailed results often makes it possible to examine specific aspects of the atomic motions far more easily than by making measurements.

In what follows, we present applications of molecular dynamics that illustrate its utility for increasing our understanding of proteins and for interpreting experiments in a more effective way.

II. Internal Motions and the Underlying Potential Surface

For native proteins with a well-defined average structure, two extreme models for the internal motions have been considered; Figure 1 provides a schematic illustration

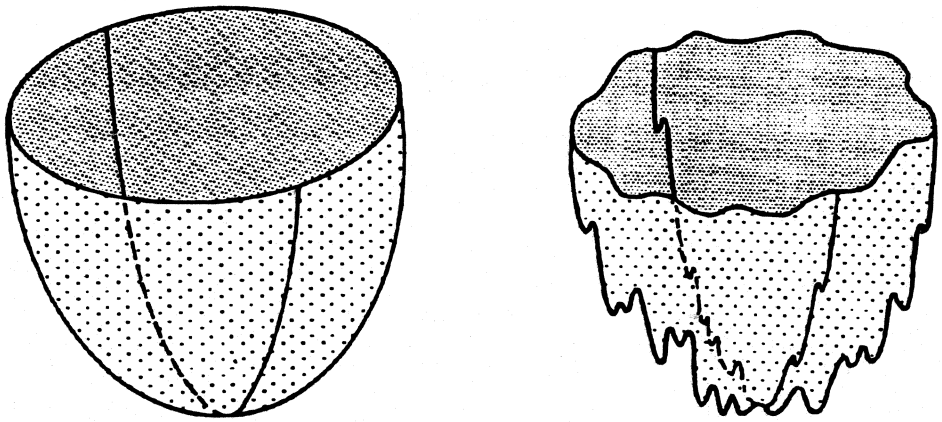

Figure 1: Schematic diagram of two potential surfaces: a) Harmonic; b) Multiple minima (substates). A two dimensional projection is used for simplicity.

of these two possibilities. In one, the fluctuations are assumed to occur within a single multidimensional well that is harmonic or quasiharmonic as a limiting case (2-4). The other model assumes that there exist multiple minima or substates; the internal motions correspond to a superposition of oscillations within the wells and transitions among them (4-9). Experimental data have been interpreted with both models, but it has proved difficult to distinguish between them (10,11).

To characterize the protein potential surface structurally and energetically, we use a 300 molecular dynamics simulation of the protein myoglobin at 300 K; details of the simulation method have been presented (12). Myoglobin was chosen for study because it has been examined experimentally by a variety of methods and the two motional models have been applied to it (5-7,10,11,13). It is ideally suited for the present analysis, because its well defined secondary structure (a series of α-helices connected by loops) facilitates a detailed characterization of the dynamics.

The topography of the potential surface underlying the dynamics can be explored by finding the local energy minima associated with coordinate sets sequential in time (14,15). Thirty-one coordinate sets (one every 10 psec) were selected and their energy was minimized with a modified Newton-Raphson algorithm suitable for large molecules (16). Since the coordinate sets all corresponded to different minima, structures separated by shorter time periods were examined to determine how long the trajectory remains in a given minimum. Seven additional coordinate sets (one every 0.05 psec) were chosen and their behavior on minimization was examined; if two coordinate sets converged, they corresponded to the same minimum; if they diverged, they corresponded to different minima (Figure 2). The measure for the distance between two structures is their rms coordinate difference after superposition. Analysis of the short time dynamics (Figure 3) demonstrates that convergence occurs for intervals up to 0.15 ± 0.05 ps. Thus, the 300 ps simulation samples on the order of 2000 different minima; this is a sizeable number but it may nevertheless be small relative to the total (finite) number of minima available to such a complex system in the neighborhood of the native average structure (that is, conformations that

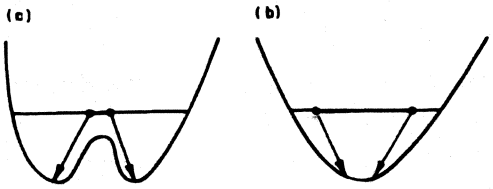

Figure 2: Schematic representation of the rms difference criterion for different minima. (a) Rms after the minimization is larger than the initial rms implying that the two conformations correspond to different minima; (b) rms after the minimization is smaller than the initial rms implying that the two conformations correspond to the same minimum.

are native-like and significantly populated at room temperature). The rms differences among the minimized structures reach a maximum value of approximately 2 Å at about 100 psec. Thus, the difference vector ($\mathbf{R}_K - \mathbf{R}_{K'}$), where $\mathbf{R}_K$ represents the coordinates of all the atoms in a native-like conformation K is restricted to a volume bounded by a radius of 2 Å.

Comparison of the energies of the minimized structures shows that the width of the energy distribution is on the order of 20K (40 cal/mole) per degree of freedom. Since the difference in energy between the "inherent" structures (14,15) is small, they are significantly populated at room temperature. Further, the large number of such structures sampled by the room temperature simulation suggests that the effective barriers separating them are low and that the protein is undergoing frequent transitions from one structure to another. The fluctuations within a well can be described by a harmonic or quasiharmonic model while the transitions among the wells cannot. Estimates based on the time development of the rms atomic fluctuations for mainchain atoms at room temperature (9) indicate that 20 to 30 percent of the rms fluctuations are contributed by oscillations within a well and 70 to 80 percent arise from transitions among wells; for sidechains the contribution from transitions among the multiple wells is expected to be larger. Since energy differences among some of the wells are small, molecules may be trapped in metastable states at low temperatures, in analogy to third law violations in crystals (e.g. crystals of CO) and models for the glassy state (11,14,15,17-19). A number of experiments suggest that the transition temperature for myoglobin is in the neighborhood of 200K (5,8,11,20). Large scale, collective motions that involve the protein surface are important in the fluctuations (9). Thus,it is possible that the observed transition is due to the freezing of the solvent matrix (9,20).

Because the details of the native structure of a protein play an essential role in its function, it is important to determine the structural origins of the multiminimum surface obtained from the dynamics analysis of myoglobin. The general features of the structure (helices and turns) are preserved throughout the simulation and the differences in position are widely distributed in the protein. The motions are associated primarily with loop displacements or relative displacements of helices which individually behave as nearly rigid bodies. Rearrangements within individual loops are the elementary step in the transition from one minimum to another; they are coupled with associated helix displacements. Which loop or turn changes in a given time interval appears to be random. Specific loop motions may be initiated by sidechain transitions in the helix contacts, mainchain dihedral angle transitions of the loops themselves, or a combination of the two. As the time interval between two structures increases, more loop transitions have occurred. At room temperature, the transition

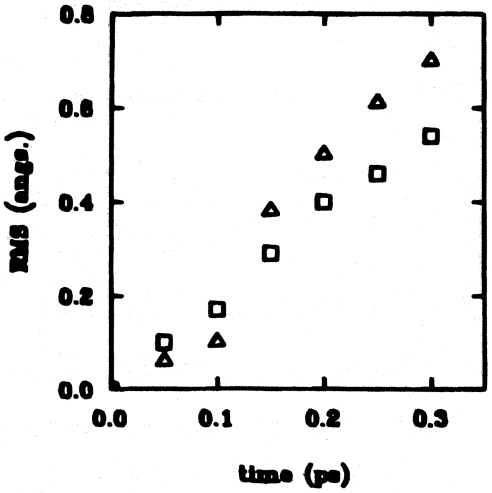

Figure 3: Root mean square difference correlation function <rms(0), rms(t)> between structures as a function of the time interval between them. Results are for 0.05 ps time interval structures; the squares are from the trajectory and the triangles are the minimized structure results.

probabilities are such that for an interval 100 psec or longer between two structures, some transitions will have taken place in all of the flexible loop regions. However, since the rms differences between structures continue to increase up to 200 psec, the configuration space available to the molecule in the 300 ps simulation includes a range of structures for the loop regions that are not completely sampled in a 100 psec.

To characterize the helix motions that are coupled with the loop rearrangements, the internal structural changes of the helices were separated from their relative motions. Individual helices and loops were superimposed and the rms differences for the mainchain calculated for the set of structures; the rms difference for the internal structure of the helices is generally less than 1 Å. The corresponding results for the loop region shows that they undergo much larger internal structural changes on the order of 2.5 Å.

In analysing the relative motion of the helices, it is of particular interest to examine the behavior of helix pairs that are in van der Waals contact; these are helix pairs A-H, B-E, B-G, F-H and G-H for all of which at least three residues from each helix are interacting. Each helix was fitted to a straight line and the fluctuations of the distance between the helix centers of mass and the relative orientations of the axes were compared. The relative translations have rms values of 0.3 to 0.7 Å and the relative rotations have rms values of 1 to 14°; the maximum differences are 1.3 to 2.2 Å and 5 to 39°, respectively.

The dynamical results for the helix motions can be compared with structural data from two sources; the first is derived from proteins of a given sequence in different environments (e.g., two different crystal forms, deoxy and oxy hemoglobin (21)) and the second from homologous proteins with different sequences (e.g., the globins (22)). The maximum dynamical displacements are somewhat larger than those observed in different x-ray structures of a given protein. The values are of the same order as the differences (2 to 3 Å, 15 to 30°; there are some larger changes) found in comparing a series of different globins with known crystal structures and sequence homologies in the range 16 to 88 percent. Thus, the range of conformations sampled by a single myoglobin trajectory is similar to that found in the evolutionary variation among structures of the globin series. This suggests that molecular plasticity is likely to have played an important role in the evolution of protein sequences.

The comparison of the various globin structures (22) indicated that the range of helix packings is achieved primarily by changes in sidechain volumes resulting from amino acid substitutions. In the dynamics, it is the correlated motions of sidechains that are in contact, plus the rearrangements of loops, that make possible the observed helix fluctuations. Different positions within wells and transitions between wells for sidechains (e.g., $\pm 60°, 180°$ for χ_1) are involved. This is in accord with the results of high-resolution x-ray studies that show significant disorder in sidechain orientations (23,24). Further, correlated dihedral angle changes differentiate the various minima. Since more than one set of sidechain orientations is consistent with a given set of helix positions, the known globin crystal structures probably represent only a small subset of the possible local minima.

Myoglobin at physiological temperature samples a very large number of different minima that arise from the inhomogenity of the system. This is expected to have important consequences for the interpretation of myoglobin function and, more generally, for the functions of other proteins, including enzymes. There are solid-like microdomains (the helices), whose mainchain structure is relatively rigid, and liquid-like regions (the loops and the sidechain clusters at interhelix contacts) that readjust as the helices move from one minimum to another. Since the minima have similar energies, myoglobin is expected to be glass-like at low temperatures. Freezing in of the liquid-like regions could result in a transition to the glassy state (19).

III. Use of Nuclear Magnetic Resonance Data for Protein Folding

Nuclear magnetic resonance (NMR) is an experimental technique that has played an essential role in the analysis of the internal motions of proteins (25-27). Like x-ray diffraction, it can provide information about individual atoms; unlike x-ray diffraction, NMR is sensitive not only to the magnitude but also to the time scales of the motions. Most nuclear relaxation processes are dependent on atomic motions on the nanosecond to picosecond time scale. Although molecular tumbling is generally the dominant relaxation mechanism for proteins in solution, internal motions contribute as well; for solids, the internal motions are of primary importance. In addition, NMR parameters, such as nuclear spin-spin coupling constants and chemical shifts, depend on the protein environment. In many cases different local confor mations exist but the interconversion is rapid on the NMR time scale, here on the order of milliseconds, so that average values are observed. When the interconversion time is on the order of the NMR time scale or slower, the transition rates can be studied by NMR; an example is provided by the reorientation of aromatic rings (28).

In addition to supplying data on the dynamics of proteins, NMR can also be used to obtain structural information. With recent advances in techniques it is now possible to obtain a large number of approximate interproton distances for proteins by the use of nuclear Overhauser effect measurements (29). If the protein is relatively small and has a well resolved spectrum, a large portion of the protons can be assigned and several hundred distances for these protons can be determined by the use of two-dimensional NMR techniques (30). Clearly, these distances can serve to provide structural information for proteins, analogous to their earlier use for organic

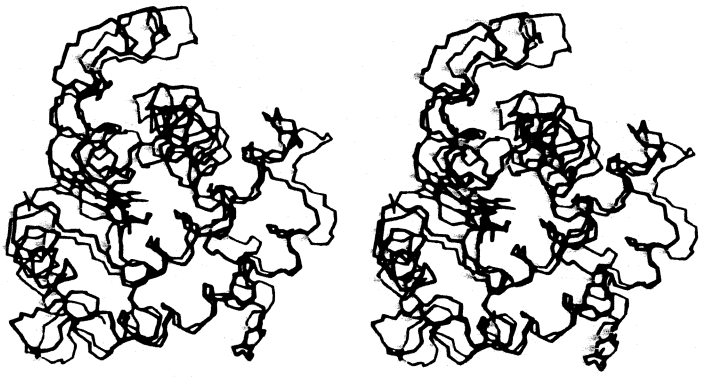

Figure 4: Minimized structures of myoglobin; stereo diagrams showing two superimposed structures separated by a time interval of 100 ps along the trajectory.

molecules (29,31). Of great interest is the possibility that enough distance information can be measured to actually determine the high resolution structure of a protein in solution. This could serve to supplement results from x-ray crystallography, particularly for proteins that are difficult to crystallize.

The nuclear Overhauser effect (NOE) corresponds to the selective enhancement of a given resonance by the irradiation of another resonance in a dipolar coupled spin system. Of particular interest for obtaining motional and distance information are measurements that provide time dependent NOE's from which the cross-relaxation rates σ_{ij} can be determined directly or indirectly by solving a set of coupled equations. Motions on the picosecond time scale are expected to introduce averaging effects that decrease the cross relaxation rates by a scale factor relative to the rigid model. A lysozyme molecular dynamics simulation (32) has been used to calculate dipole vector correlation functions (33) for proton pairs whose distance is not fixed by the structure of a residue. The results show that the presence of these motions will cause a general decrease in most NOE effects observed in a protein. However, because the distance depends on the sixth root of the observed NOE, motional errors of a factor of two in the latter lead to only a 12% uncertainty in the distance. Thus, the decrease is usually too small to produce a significant change in the distance estimate from the measured NOE value. This is consistent with the excellent correlation found between experimental NOE values and those calculated using distances from a crystal structure (34). Specific NOE's can, however, be altered by the internal motions to such a degree that the effective distances obtained are considerably different from those predicted for a static structure. Such possibilities must, therefore, be considered in any structure determination based on NOE data. This is true particularly for cases involving averaging over large scale fluctuations.

Because of the inverse sixth power of the NOE distance dependence, experimental data so far are limited to protons that are separated by less than 5 Å. Thus, the information required for a direct protein structure determination is not available. To overcome this limitation it is possible to introduce additional information provided by empirical energy functions (16). One way of proceeding is to do molecular

dynamics simulations with the approximate interproton distances introduced as restraints in the form of skewed biharmonic potentials (35,36) with the force constants chosen to correspond to the experimental uncertainty in the distance.

A model study of the small protein crambin, which is composed of 46 residues, was made with realistic NOE restraints (36). Two hundred forty approximate interproton distances less than 4 Å were used, including 184 short-range distances (i.e., those connecting protons in two residues that are less than 5 residues apart in the sequence) and 56 long-range distances. The molecular dynamics simulations converged to the known crambin structure (37) from different initial extended structures. The average structure obtained from the simulations with a series of different protocols had rms deviations of 1.3 Å for the backbone atoms, and 1.9 Å for the sidechain atoms. Individual converged simulations had rms deviations in the range 1.5 to 2.1 Å and 2.1 to 2.8 Å for the backbone and sidechain atoms, respectively. Further, it was shown that a dynamics structure with significantly large deviations (5.7 Å) could be characterized as incorrect, independent of a knowledge of the crystal structure because of its higher energy and the fact that the NOE restraints were not satisfied within the limits of error. The incorrect structure resulted when all NOE restraints were introduced simultaneously, rather than allowing the dynamics to proceed first in the presence of only the short-range restraints followed by introduction of the long-range restraints. Also of interest is the fact that although crambin has three disulfide bridges it was not necessary to introduce information concerning them to obtain an accurate structure.

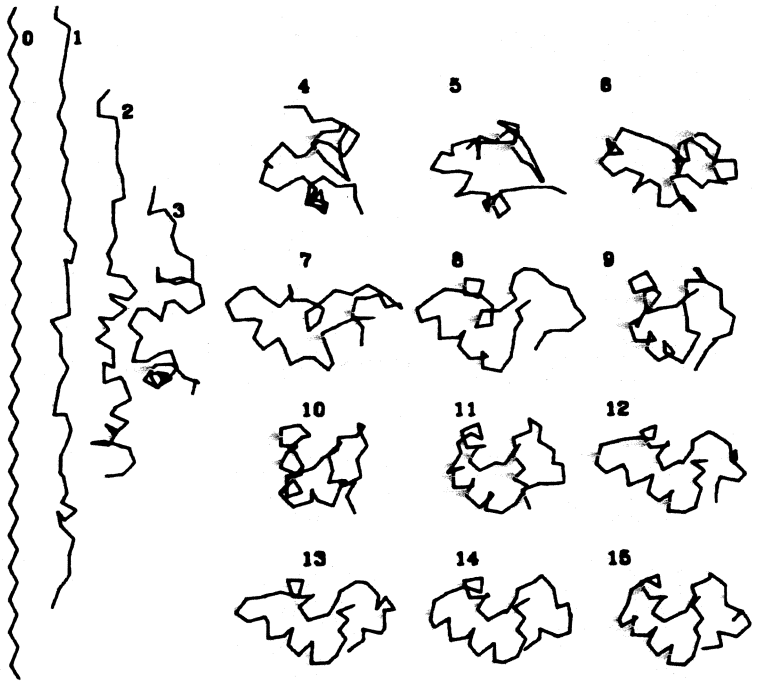

Figure 5: Folding of crambin backbone by restrained molecular dynamics. Starting with the initial structure snapshots are shown at 1 ps intervals; only the C^{α} backbone is included in the figure.

The folding process as simulated by the restrained dynamics is very rapid (see Figure 5). At the end of the first 2 ps the secondary structure is essentially established while the molecule is still in an extended conformation. Some tertiary folding occurs even in the absence of long-range restraints. When they are introduced, it takes about 5 ps to obtain a tertiary structure that is approximately correct and another 6 ps to introduce the small adjustments required to converge to the final structure.

It is of interest to consider the relation between the results obtained in the restrained dynamics simulation and actual protein folding. That correctly folded structures are achieved only when the secondary structural elements are at least partly formed before the tertiary restraints are introduced is suggestive of the diffusion-collision model of protein folding (38). Clearly, the specific pathway has no physical meaning since it is dominated by the NOE restraints. Also, the time scale of the simulated folding process is 12 orders of magnitude faster than experimental estimates. About 6 to 9 orders of magnitude of the rate increase are due to the fact that the secondary structure is stable once it is formed, in contrast to real protein folding where the secondary structural elements spend only a small fraction of time in the native conformation until coalescence has occurred. The remainder of the artificial rate increase presumably arises from the fact that the protein follows a single fairly direct path to the folded state in the presence of the NOE restraints, instead of having to go through a complex search process.

IV X-Ray Refinement by Simulated Annealing

Crystallographic structure determinations by x-ray or neutron diffraction generally proceed in two stages. First, the phases of the measured reflections are estimated and a low- to medium-resolution model of the protein is constructed and second, more precise information about the structure is obtained by refining the parameters of the molecular model against the crystallographic data (39). The refinement is performed by minimizing the crystallographic R factor, which is defined as the difference between the observed ($|F_{obs}(h,k,l)|$) and calculated ($|F_{calc}(h,k,l)|$) structure factor amplitudes,

$$R = \sum_{h,k,l} |F_{obs}(h,k,l)| - |F_{calc}(h,k,l)| \Big/ \sum_{h,k,l} |F_{obs}(h,k,l)| \qquad [1]$$

where h,k,l are the reciprocal lattice points of the crystal.

Conventional refinement involves a series of steps, each consisting of a few cycles of least-squares refinement with stereochemical and internal packing constraints or restraints (40-43) that are followed by manual rebuilding of the model structure by use of interactive computer graphics. Finally, solvent molecules are included and alternative conformations for some protein atoms may be introduced. The standard refinement procedure is time consuming, because the limited radius of convergence of least-squares algorithms (approximately 1 Å) necessitates the periodic examination of electron density maps computed with various combinations of F_{obs} and F_{calc} as amplitudes, and with phases calculated from the model structure. Also, the least-

squares refinement process is easily trapped in a local minimum so that human intervention is necessary.

Simulated annealing (44), which makes use of Monte Carlo or molecular dynamics (45) simulations to explore the conformational space of the molecule can help to overcome the local-minimum problem. This has been demonstrated in the application of molecular dynamics to structure determination with nuclear magnetic resonance (NMR) data (see Sect. III). In contrast to the NMR application (36), the initial model for crystallographic refinement cannot be arbitrary. It has to be relatively close to the correct geometry to provide an adequate approximation to the the structure factors.

To employ molecular dynamics in crystallographic refinement, an effective potential

$$E_{sf} = S \sum_{h,k,l} [|F_{obs}(h,k,l)| - |F_{calc}(h,k,l)|]^2 \qquad [2]$$

was added to the empirical potential energy function (16). The effective potential E_{sf} describes the differences between the observed structure factor amplitudes and those calculated from the atomic model; it is identical to the function used in standard least-squares refinement methods (41). The scale factor S was chosen to make the gradient of E_{sf} comparable in magnitude to the gradient of the empirical energy potential of a molecular dynamics simulation with S set to zero.

As in the case of the NMR analysis (see Sect. III), simulated annealing refinement was also tested on crambin, for which high-resolution x-ray diffraction data and a refined structure, determined by resolved anomalous phasing and conventional least-squares refinement with model-building, are available (37). The initial structure for the MD-refinement was obtained from the NMR structure determination; the orientation and position of the NMR-derived crambin molecule in the unit cell was determined by molecular replacement (46). The root-mean-square (rms) differences for residue positions of this initial structure and the final manually refined structure (37) are as large as 3.5 Å, with particularly large differences for residues 34 to 40; the R factor of the initial structure was 0.56 at 2 Å resolution. MD-refinement at 3000°K starting with 4 Å resolution data for 2.5 ps, extending to 3 Å resolution for 2.5 ps, and finally to 2 Å resolution for 5 ps, followed by several cycles of minimization, reduces the atomic rms deviations to 0.34 and 0.56 Å for the backbone and side chain atoms, respectively. During the MD-refinement, some atoms in residues 35 to 40 moved by more than 3 Å. The essential point is that the refinement of the crambin structure was achieved starting from the initial NMR-structure without human intervention. The R factor (0.294) of the MD-refined structure is somewhat higher than the R factor (0.258) of the manually refined structure without solvent and with constant temperature factors; minor model-building would correct this difference. Other annealing protocols using higher temperatures (e.g., 7000 to 9000K yield structures that are still closer to the manually refined structure. The refinement required approximately one hour of central processing unit (CPU) time on a CRAY-1; structure factor calculations accounted for about half this time. The latter portion of the calculation has been considerably reduced in

time by use of Fast Fourier transform (FFT) methods (A. Brünger, to be published).

As a control, the initial NMR-derived structure was refined without rebuilding by a restrained least-squares method (42), starting at 4 Å resolution and then increasing the resolution to 3 Å, and finally to 2 Å. The R factor dropped to 0.381, but the very bad stereochemistry and large deviation from the manually refined structure indicate that this structure has not converged to the correct result; residues 34 to 40 have not moved and substantial model-building would be required to correct the structure. Thus, restrained least-squares refinement in the absence of model-building did not produce the large conformational changes that occurred in MD-refinement by simulated annealing.

V. Conclusion

Molecular dynamics is now playing an important role in the study of the properties of macromolecules of biological interest. It can also be used effectively in the analysis of experimental data and has been shown to provide an approach to structure determination by NMR and by x-ray crystallography. Because molecular dynamics simulations are relatively new they have so far been employed primarily by theoreticians. It is to be hoped that in the not-too-distant future experimentalist will also use molecular dynamics as a research tool for obtaining a deeper understanding of the biomolecules with which they work.

Acknowledgements

We wish to thank our collaborators who have contributed to the work described here. They include G.M. Clore, C.M. Dobson, A.M. Gronenborn, T. Ichiye, R.M. Levy, E.T. Olejniczak, and G.A. Petsko. The work was supported in part by grants from the National Science Foundation and the National Institutes of Health. This paper is a slightly abbreviated version of a contribution made to the Cold Spring Harbor Symposium in May, 1987.

References

1. C.B. Brooks III, M. Karplus, and B.M. Pettitt, *Adv. Chem. Phys.* (John Wiley & Sons, New York, to be published.
2. M. Karplus and J.N. Kushick, *Macromolecules 14*, 325 (1981).
3. M. Levitt, C. Sander, and P.S. Stern, *J. Mol. Biol. 181*, 423 (1985).
4. B.R. Brooks and M. Karplus, *Proc. Natl. Acad. Sci. USA 80*, 6571 (1983).
5. R.H. Austin, K.W. Beeson, L. Eisenstein, H. Frauenfelder, and I.C. Gunsalus, *Biochemistry 14*, 5355 (1975).
6. H. Frauenfelder, G.A. Petsko, and D. Tsernoglou, *Nature 280*, 558 (1979).
7. R.M. Levy, D. Perahia, and M. Karplus, *Proc. Natl. Acad. Sci. USA 79*, 1346 (1982).
8. P.G. Debrunner and H. Frauenfelder, *Ann. Rev. Phys. Chem. 33*, 283 (1982).
9. S. Swaminathan, T. Ichiye, W.F. van Gunsteren, and M. Karplus, *Biochemistry 21*, 5230 (1982).
10. M. Agmon and J.J. Hopfield, *J. Chem. Phys. 79*, 2042 (1983).
11. A. Ansari, J. Berendzen, S.F. Bowne, H. Frauenfelder, I.E.T. Iben, T.B. Sauke, E. Shyamsunder, and R.D. Young, *Proc. Natl. Acad. Sci. USA 82*, 5000 (1985).
12. R.M. Levy, R.P. Sheridan, J.W. Keepers, G.S. Dubey, S. Swaminathan, and M. Karplus, *Biophys. J. 48*, 509 (1985)

13. W. Bialek, and R.F. Goldstein, *Biophys. J. 48*, 1027 (1985).
14. F. H. Stillinger and T. A. Weber, *Phys. Rev. A25*, 978 (1982).
15. F.H. Stillinger and T.A. Weber, *Science 225*, 983 (1984).
16. B.R. Brooks, B.R., R.E. Bruccoleri, B.D. Olafson, D.J. States, S. Swaminathan, and M. Karplus, *J. Comp. Chem. 4*, 187 (1983).
17. J.M. Ziman, *Models of Disorder*, Sect.7.2 (Cambridge University Press, 1979). 978 (1982).
18. G. Toulouse, *Helv. Phys. Acta 57*, 459 (1984).
19. D.L. Stein, *Proc. Natl. Acad. Sci. USA 82*, 3670 (1985).
20. F. Parak, E.W. Knapp, and D. Kucheida, *J. Mol. Biol. 161*, 177 (1982).
21. C. Chothia and A.M. Lesk, *TIBS 10*, 116 (1985).
22. A.M. Lesk and C. Chothia, *J. Mol. Biol. 136*, 225 (1980).
23. J.L. Smith, W.A. Hendrickson, R.B. Honzatko, and S. Sheriff, *Biochemistry 25*, 5018 (1986).
24. J. Kuriyan, M. Karplus, and G.A. Petsko, *Proteins*, 2,1 (1987).
25. I.D. Campbell, C. M. Dobson, and R.J.P. Williams, *Adv. Chem. Phys. 39*, 55 (1978).
26. F.R.N. Gurd and J.M. Rothgeb, *Adv. Prot. Chem. 33*, 73 (1979).
27. M. Karplus and J.A. McCammon, *CRC Crit. Rev. Biochem. 9*, 293 (1981).
28. I.D. Campbell, C.M. Dobson, G.R. Moore, S.J. Perkins, and J.P. Williams, *FEBS Lett. 70*, 96 (1976).
29. J.H. Noggle and R.E. Schirmer, *The Nuclear Overhauser Effect*, (Academic Press, New York, 1971).
30. G. Wagner and K. Wüthrich, *J. Mol. Biol. 160*, 343 (1982).
31. B. Honig, B. Hudson, B.D. Sykes, and M. Karplus, *Proc. Natl. Acad. Sci. USA 68*, 1289 (1971).
32. T. Ichiye, B.D. Olafson, S. Swaminathan, and M. Karplus, *Biopolymers 25*, 1909 (1986).
33. E.T. Olejniczak, C.M. Dobson, R.M. Levy, and M. Karplus, *J. Am. Chem. Soc. 106*, 1923 (1984).
34. F.M. Poulsen, J.C. Hoch, and C.M. Dobson, *Biochemistry 19*, 2597 (1980).
35. G.M. Clore, A.M. Gronenborn, A.T. Brünger, and M. Karplus, *J. Mol. Biol. 186*, 435 (1985).
36. A.T. Brünger, G.M. Clore, A.M. Gronenborn, and M. Karplus, *Proc. Natl. Acad. Sci. USA. 83*, 3801 (1986).
37. W.A. Hendrickson and M.M. Teeter, *Nature (London) 290*, 107 (1981).
38. D. Bashford, D.L. Weaver, and M. Karplus, *J. Biomol. Str. Dyn. 1*, 1243 (1984).
39. H.W. Wyckoff, C.H.W. Hirs, and S.N. Timasheff, Eds., *Methods Enzymol. 115*, Part B (1985).
40. J.L. Sussman, S.R. Holbrook, G.M. Church, S.-H. Kim, *Acta Cryst. A33*, 800 (1977).
41. A. Jack and M. Levitt, *Acta Cryst. A34*, 931 (1978).
42. J.H. Konnert and W.A. Hendrickson, *Acta Cryst. 36*, 344 (1980).
43. D.S. Moss and A.J. Morffew, *Comput. & Chem. 6*, 1 (1982).
44. S. Kirkpatrick, C.D. Gelatt, Jr., M. P. Vecchi, *Science 220*, 671 (1983).
45. A.T. Bruünger, J. Kuriyan, and M. Karplus, *Science 235*, 458 (1987).
46. A.T. Bruünger, R.L. Campbell, G.M. Clore, A.M. Gronenborn, M. Karplus, G.A. Petsko, and M.M. Teeter, *Science 235*, 1049 (1987).